Catalysis Today 144 (2009) 13–18

Contents lists available at ScienceDirect

Catalysis Today

journal homepage: www.elsevier.com/locate/cattod

Ce-doped TiO_2 for photocatalytic degradation of chlorophenol

Adrián M.T. Silva [a,*], Cláudia G. Silva [a], Goran Dražić [b], Joaquim L. Faria [a,*]

[a] Laboratório de Catálise e Materiais (LCM), Laboratório Associado LSRE/LCM, Departamento de Engenharia Química, Faculdade de Engenharia, Universidade do Porto, Rua Dr. Roberto Frias, 4200-465 Porto, Portugal
[b] Jozef Stefan Institute, Department of Nanostructured Materials, Jamova 39, SI-1000 Ljubljana, Slovenia

ARTICLE INFO

Article history:
Available online 25 March 2009

Keywords:
Photocatalysis
Titanium dioxide
Cerium
Doping
Visible-light
4-Chlorophenol

ABSTRACT

Visible-light photoactive Ce-doped TiO_2 catalysts are prepared by solvothermolysis, characterized by several techniques (DRIFT, DR UV–vis, XRD and HRTEM/SAED/EDXS) and tested in the degradation of 4-chlorophenol. TiO_2 materials are modified with low amounts of cerium to extend its absorption spectrum into the visible region. The presence of cerium, in an excess of 0.6% (w/w), is found to inhibit the transition from amorphous to crystalline phase during calcination at 400 °C. The observed photocatalytic activity is strongly dependent on both visible-light response and structure of the material. Cerium has a positive effect in preventing electron–hole recombination only when the crystalline structure is maintained. Compared with the commercial P-25 TiO_2 catalyst, the activity observed at the initial period of the reaction is higher for the prepared Ce-doped material. However, in the case of the latter catalyst, activity decreases after 15 min in an experiment carried out at natural pH (5.8). This decrease in activity is not observed for a higher pH value (10) and seems to be related with catalyst deactivation due to removal of ceria from the surface. Finally, in the case of Ce-doped TiO_2 materials, the main intermediates of degradation are hydroquinone and benzoquinone, while with P-25 the main intermediate is 4-chlorocatechol, suggesting that different reaction mechanisms may take place depending on the nature of the catalyst.

1. Introduction

Some of the important challenges of this decade include overall reduction of human exposure to chemical pollutants and minimization of human impact in sensitive eco-systems and biodiversity [1]. Hazardous water soluble phenolic compounds are continuously introduced in the environment through domestic and industrial activities, representing a severe toxicological risk. Nowadays, photochemical degradation of phenol derivatives represents an effective alternative to biological detoxification. Heterogeneous photocatalysis involving TiO_2 has been systematically reviewed at fundamental and applied levels [2–7]. Commercial worldwide interest in this technology is explicit, but is still in pilot, or lab development, in most cases. The process fundamentals consist in hitting the semiconductor with radiation of energy near to, or greater than its band gap energy, generating high energy electron–hole pairs, which initiate the heterogeneous photocatalytic reaction. However, undesirable recombination of electrons and holes, and low efficiency under irradiation in the visible region are the two main drawbacks associated with the use of non-modified TiO_2.

To overcome these limitations, one possible solution consists in doping the TiO_2 semiconductor with d-metal ions/oxides [8–10]. In particular, cerium oxides have attracted much attention due to the optical and catalytic properties associated to the redox pair Ce^{3+}/Ce^{4+}. Ce-doped TiO_2 materials have been preferentially prepared by the sol–gel and hydrothermal methods [8,10–15] and tested in the photodegradation of a variety of model pollutants, such as Rhodamine B [10,12,15], methyl orange [9], formaldehyde [14] and 2-mercaptobenzothiazole [8]. Unlike the situation concerning other photocatalysts, only few works deal with Ce-doped catalysts. The actual oxidation mechanism involved in these reactions is still uncertain and a limited number of photodegradation mechanisms have been tentatively proposed in the literature [8,10,13]. Moreover, the beneficial effect of Ce-doped TiO_2 catalysts depends on different factors, such as the synthesis method and the Ce content. For instance, in experiments with Rhodamine B, both positive [10] and negative [12] effects were observed when TiO_2 was doped with Ce, while some relative efficiency was attributed to the type of crystalline phase [15]. The possible partial blockage of the surface sites and the decrease in the number of surface groups are some disadvantages when doping TiO_2 with Ce [12], while light-response in the visible region and electron–hole separation are some common advantages [8,10].

* Corresponding authors. Tel.: +351 225081998; fax: +351 225081449.
E-mail addresses: adrian@fe.up.pt (Adrián M.T. Silva), jlfaria@fe.up.pt (J.L. Faria).

0920-5861/$ – see front matter © 2009 Elsevier B.V. All rights reserved.
doi:10.1016/j.cattod.2009.02.022

In the present work, we prepared Ce-doped TiO_2 photocatalysts by solvothermolysis with different loads of cerium. The prepared materials were characterized by spectroscopic (DRIFTS, DR UV–vis), electron microscopic (HRTEM/SAED/EDXS, HAADF/TEM) and X-ray diffraction (XRD) analysis. The materials were tested in the degradation of 4-chlorophenol (4-CP), which was chosen as probe molecule, due to its environmental importance as priority toxic pollutant [16]. To the best of our knowledge, this is the first work reporting the photocatalytic oxidation of this compound with Ce-doped TiO_2 materials.

2. Experimental

2.1. Reagents and materials

Cerium(III) nitrate hexahydrate ($Ce(NO_3)_3{\cdot}6H_2O$, 99%), titanium (IV) isopropoxide ($Ti[OCH(CH_3)_2]_4$, 97%), 4-chlorophenol (ClC_6H_4OH ≥99%), hydroquinone ($C_6H_4(OH)_2$, 99%), benzoquinone ($C_6H_4(O)_2$, 99.5%), 4-chlorocatechol ($ClC_6H_3(OH)_2$, 97%) and potassium hydroxide (KOH) were supplied by Sigma–Aldrich. Acetonitrile (≥99.8%) and methanol (≥99.8%) were used with a HPLC grade (Chromanorm), while ethanol (99.5%) was obtained from Panreac. Ultrapure water was produced in a Direct-Q millipore system. TiO_2 Aeroxide P-25 was supplied by Degussa AG (now Evonik).

2.2. Catalyst preparation

Ce-doped TiO_2 materials with different mass percentages of cerium (0.2, 0.4, 0.6, 0.8 and 1.0% (w/w)) were prepared by solvothermolysis, using cerium(III) nitrate and titanium(IV) isopropoxide as precursors (hereafter named as Ce*X.X*Ti–O, where *X.X* stands for metal load) and methanol as solvent. The main role of the organic solvent is to act as an oxygen source for the metal oxide formation. In a typical synthesis procedure, 2.4 mL of titanium precursor was added to 75 mL of pure methanol, at room temperature under continuous stirring and in alkaline media adjusted by using KOH (3 M). Subsequently, the proper amount of hydrated cerium nitrate was slowly dissolved in this solution, under stirring for 30 min, in order to obtain a homogeneous solution. The final solution was transferred to a 250-mL temperature controlled glass-container, immersed in an oil bath, heated up to 75 °C under normal pressure, and kept at this temperature for 21 h, for solvothermal treatment. At the end of this period, the autoclave was cooled to room temperature. The precipitates obtained were separated from the liquor by centrifugation, washed thoroughly with deionized water and ethanol, dried at 100 °C overnight, and calcined in air atmosphere at 400 °C for 2 h, in an horizontal tubular oven. The solid was heated at 5 °C min^{-1}, from room temperature to 150 °C, kept at this temperature for 30 min and then heated again at 5 °C min^{-1} up to 400 °C. The absence of potassium in selected samples was confirmed by EDXS. Bare TiO_2 was synthesized using the same approach, but without adding the cerium precursor.

2.3. Photocatalytic experiments

The batch photochemical degradation experiments were conducted in a glass-immersion photochemical reactor (250 mL) equipped with a UV–vis Heraeus TQ 150 medium pressure mercury lamp. An optical cut-off of UVB and UVC lights was created with a glass jacket (main resulting emission lines: 366, 405 and 436 nm). The initial concentration of 4-CP was 100 mg/L (natural pH = 5.8). Catalyst concentration was set at 1 g/L. A 200 mL min^{-1} oxygen/argon (20 vol.% of oxygen) stream was continuously supplied to the reactor. Before turning on the lamp, the suspensions were saturated with the gas mixture and magnetically stirred for 30 min to establish an adsorption–desorption equilibrium. Then, the suspensions were irradiated at constant stirring speed. Samples were withdrawn regularly from the reactor and centrifuged prior to analysis, in order to separate any suspended solids. Conversions were calculated in relation to initial 4-CP concentration.

2.4. Analytical techniques

Diffuse Reflectance Infrared Fourier Transform Spectroscopy (DRIFTS) was performed in a Nicolet 510P spectrophotometer equipped with a diffuse reflectance attachment (4000–400 cm^{-1}; 256 scans, resolution 4 cm^{-1}) under ambient conditions. The instrument software converted the diffuse reflectance spectra to equivalent absorption Kubelka–Munk units, which express the peak intensity calculated from the reflectance of a diluted sample of infinite depth upon application of the Kubelka–Munk mathematical function. The Diffuse Reflectance Ultraviolet–visible (DR UV–vis) spectra of the powder catalysts were recorded on a JASCO V-560 UV–vis spectrophotometer, with a double-monochromator/double-beam optical arrangement, equipped with an integrating sphere attachment (JASCO ISV-469). The powders were not diluted in any matrix to avoid decrease of the absorbance. The reflectance spectra were converted by the instrument software (JASCO) to equivalent absorption Kubelka–Munk units.

A JEOL 2010F analytical electron microscope, equipped with a field-emission gun was used for High-Resolution Transmission Electron Microscopy (HTREM) investigations. Microscope was operated at 200 kV and an Energy-Dispersive X-ray Spectrometer (EDXS) LINK ISIS-300 from Oxford Instruments, equipped with an UTW Si–Li detector, was employed for the chemical analysis. Z-contrast images were collected using a High-Angle Annular Dark-Field Detector (HAADF) in Scanning Transmission Mode (STEM). For determination of the crystals structure Selected Area Electron Diffraction (SAED) technique was used. X-ray Diffraction (XRD) analysis was carried out in a Philips X'Pert MPD rotator target diffractometer (λ = 0.15406 nm, 40 kV; data recorded at a 0.017° step size) in order to determine the phase composition and calculate the crystallite size from the XRD diffraction peaks (using the Scherrer equation). BET surface area was determined at 77 K with an automatic analyzer Quantachrom NOVA 4200e, using the N_2 adsorption isotherm.

The concentration of each species was followed by High Performance Liquid Chromatography (HPLC) using a computer-controlled Hitachi Elite LaChrom HPLC system, equipped with a Diode Array Detector (L-2450) and a solvent delivery pump (L-2130), at a flow rate of 1 mL/min. 4-CP and its reaction intermediates were detected using a Hydrosphere C18 column (250 mm × 4.6 mm; 5 μm particles) with a gradient method. At first, the column was equilibrated with a A:B (70:30) mixture of 20 mM NaH_2PO_4 acidified with H_3PO_4 at pH = 2.80 (A) and acetonitrile (B), followed by a linear gradient run to A:B (30:70) in 13 min and finally with isocratic elution during 2 min. Quantification was based on the chromatograms taken by measuring the concentration of each compound at their maximum absorbance value and using the EZChrom Elite chromatography data handling software (Version 3.1.7). Absorbance was found to be linear over the whole range considered (maximum relative standard deviation of 2%). The concentration of chloride ions was determined by ion chromatography using a Dionex DX-120 Chromatograph equipped with a Dionex AS9-HC column.

3. Results and discussion

3.1. Ce–TiO_2 catalysts characterization

The DRIFT spectra of the materials synthesized in the laboratory and calcined at 400 °C, namely bare and Ce-doped TiO_2 catalysts

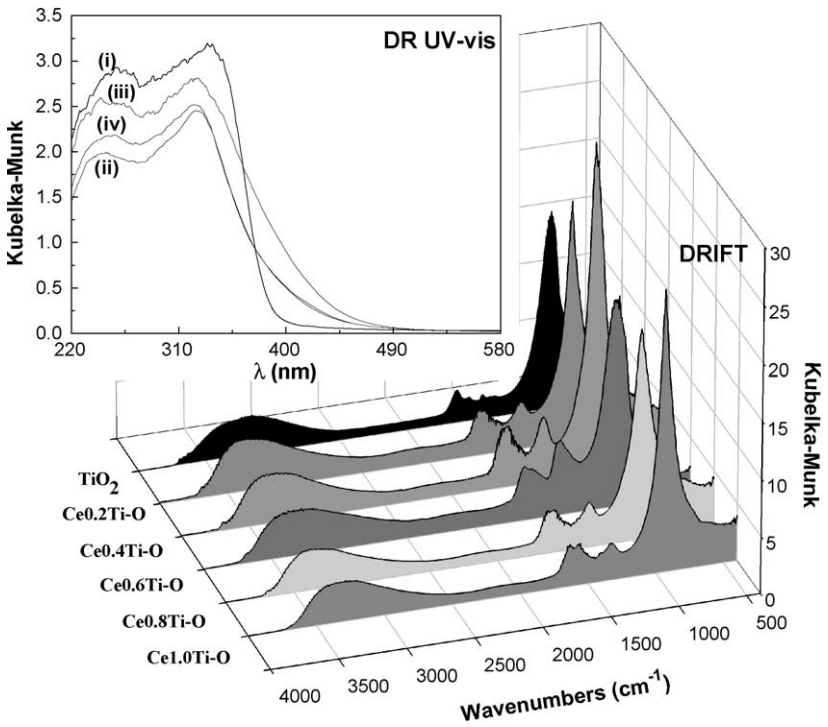

Fig. 1. DRIFT spectra of bare TiO_2 and Ce-doped TiO_2 catalysts (Ce*X*.*X*Ti–O) prepared with different amounts of Ce (*X*.*X* = 0.2–1.0%, w/w). Inset: DR UV–vis spectra of (i) TiO_2, (ii) Ce0.2Ti–O, (iii) Ce0.6Ti–O, and (iv) Ce0.8Ti–O.

with different amounts of Ce are shown in Fig. 1. The main band related to TiO_2 (944 cm^{-1}) is visible in all spectra. The band appearing in the nearby region (1400 cm^{-1}) has been attributed to the NO_3^- groups [13] from the cerium precursor, which is not present in the undoped TiO_2. The band between 2500 and 3800 cm^{-1} with maximum ca. 3383 cm^{-1} and the two bands appearing at 1585 and 1633 cm^{-1}, correspond to the stretching vibration of hydroxyl groups (O–H) and hydrogen-bonded surface water molecules [17] in coordinated water, Ti–OH groups, or other hydrated species. The peak of TiO_2 rutile crystalline phase, typically observed ca. 490 cm^{-1} (Ti–O vibration) was not observed in the Ce-doped TiO_2 samples. This was expected, since the transformation from anatase to rutile crystalline phase, in bare TiO_2, usually starts at temperatures higher than 400 °C [18] and is retarded when TiO_2 is doped with cerium ions [11].

Regarding the DR UV–vis spectra of representative samples shown in Fig. 1 inset, is noticeable that bare TiO_2 absorbs at wavelengths shorter than 400 nm. With the introduction of cerium, the absorption edge shifts towards longer wavelengths (400–500 nm), thus extending absorption into the visible region. The shift is greater when doping TiO_2 with 0.6% (w/w) Ce, when compared to others. This red-shift of the absorption edge in Ce–TiO_2 catalysts has been attributed to the Ce 4f level [8,10], promoting the generation of electron–holes under visible-light irradiation.

Fig. 2 shows the HRTEM images of a selected zone in Ce0.6Ti–O catalyst, where the CeO_2 phase is clearly identified, as confirmed

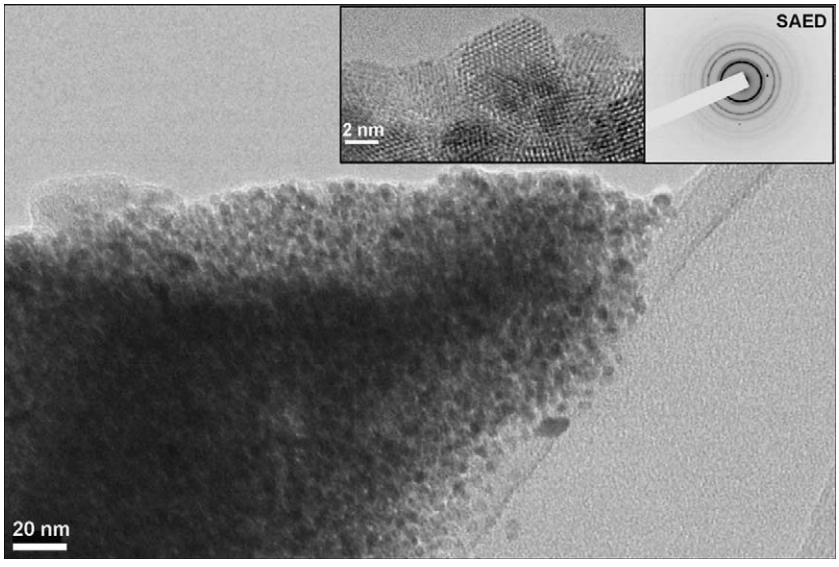

Fig. 2. CeO_2 phase observed by HRTEM of the Ce0.6Ti–O catalyst (inset: HRTEM at higher magnification and SAED pattern).

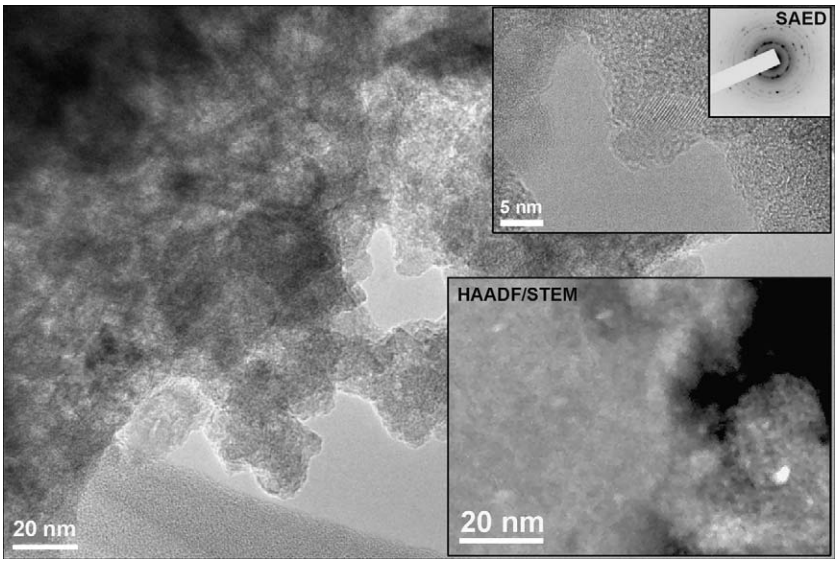

Fig. 3. TiO_2 phase observed by HRTEM of the Ce0.6Ti–O catalyst (inset: HRTEM at higher magnification, SAED pattern and HAADF/STEM image Z-contrast).

by the correspondent SAED pattern (see inset) characteristic for cubic CeO_2. This CeO_2 phase consists of clearly cut nano-crystals in the nanometer range (~5 nm sized particles), as seen in the HRTEM inset image. Some titanium was detected in the EDXS spectra (not shown), but can only be derived from TiO_2 neighbour particles. Observing the HRTEM image of the TiO_2 phase (Fig. 3) and the respective SAED pattern, 5–10 nm anatase particles are identified, and practically no evidence of Ce was found, probably due to the small amount of cerium contained in the sample (0.6%, w/w). However, using HAADF/STEM (Z-contrast image, Fig. 3 inset), bright Ce-particles (~5 nm in size) can be observed in the TiO_2 phase.

HRTEM/SAED/EDXS analyses of bare TiO_2 and Ce1.0Ti–O were also performed (not shown). Bare TiO_2 consists of small crystals (up to 10 nm) which were identified as anatase by SAED. In contrast, Ce1.0Ti–O is mostly amorphous, with faint anatase rings seen by SAED. It can be concluded that doping of TiO_2 with cerium ions restrains the transition amorphous structure to crystalline anatase, therefore increasing this transition phase temperature. These observations are clearly supported by XRD (Fig. 4), since crystallinity decreases as follows: TiO_2 > Ce0.6Ti–O > Ce1.0Ti–O. For bare TiO_2, the 2θ diffraction peaks at 25.3°, 37.8°, 47.6° and 54.1° [13] correspond to anatase crystalline phase. The size of the crystallites calculated from the diffractograms is 7 nm, which is in accordance with the HRTEM/SAED observations.

As previously observed, in the Ce0.6Ti–O sample we can identify two separate phases: cubic CeO_2 (Fig. 2); and TiO_2 anatase crystalline form (Fig. 3). Regarding the amorphous Ce1.0Ti–O sample, a broad peak was observed at ca. $2\theta = 30°$ by XRD. A similar peak, centred at $2\theta = 30.6°$, was also observed by Xie and Yuan [13] when preparing Ce-doped TiO_2 materials, using chemical coprecipitation–peptization and hydrothermal approaches. These authors attributed it to cerium titanate–$Ce_xTi_{(1-x)}O_2$. Therefore, in the Ce-doped TiO_2 materials, cerium can be present as separated cubic CeO_2, or as cerium titanate in the TiO_2 phase.

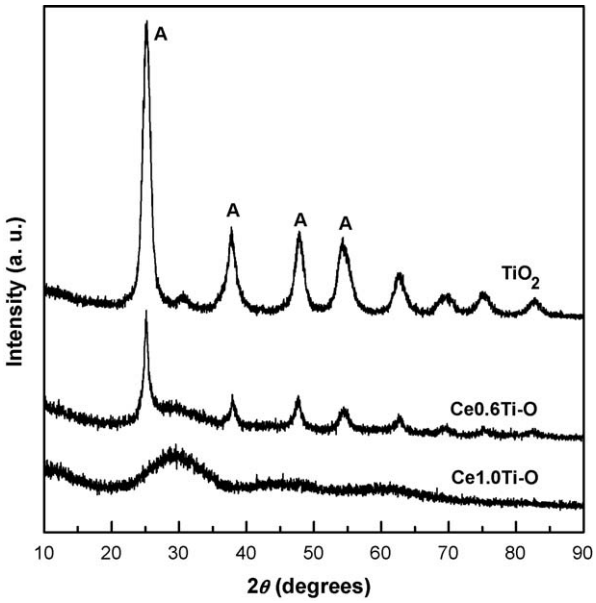

Fig. 4. XRD patterns of bare and Ce-doped TiO_2 catalysts.

3.2. Effect of different Ce loadings on TiO_2 photocatalytic activity

The concentration *vs.* time profiles of 4-CP conversion under visible-light irradiation using the different catalysts are presented

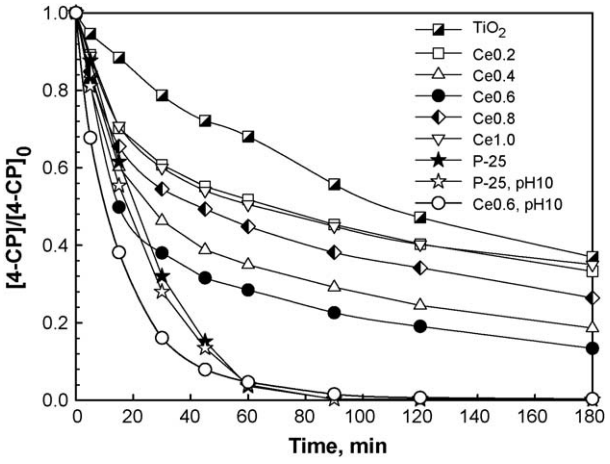

Fig. 5. Degradation *vs.* time decay curves of 4-CP during the photocatalytic experiments using different catalysts at natural pH (5.8) or adjusted to a pH value of 10 (when indicated by the figure label).

in Fig. 5. TiO_2 synthesized by the solvothermal procedure is rather inefficient. Moreover, the phenolic compound is poorly degraded by direct photolysis (results not shown). However, when Ce is introduced there is a pronounced increase in the degradation rate of 4-CP. Since cerium extends the photoresponse into the visible region, this can lead to an increase in the charge separation efficiency of surface electron–hole pairs. The redox pair of cerium (Ce^{3+}/Ce^{4+}) is also important, since cerium could act as an effective electron scavenger to trap the bulk electrons in TiO_2.

The results of Fig. 5 also show that the effectiveness of the catalyst is strongly dependent on the loading of Ce. The 4-CP conversion at 180 min, at natural pH, follows the order: Ce0.6% (86.6%) > Ce0.4% (81.4%) > Ce0.8% (73.6%) > Ce0.2% (66.7%) > Ce1.0% (65.0%). Thus, the photocatalytic efficiency increases with cerium content increase up to the optimum Ce doping concentration of 0.6% (w/w). For higher cerium contents, it was observed that the transition of the TiO_2 amorphous structure to the anatase crystalline phase is inhibited. Therefore, the decrease in the photocatalytic activity for Ce > 0.6% (w/w) can be due to the presence of amorphous phase in the resulting catalyst, promoting electron–hole recombination.

3.3. Ce–TiO_2 vs. TiO_2 P-25

For comparison purposes, we used the commercial P-25 TiO_2 catalyst (consisting of 80% anatase and 20% rutile). Previous studies have shown that this low cost and relatively stable material is very effective for the photocatalytic degradation of various phenolic compounds [19–21], including 4-CP [21]. The results are shown in Fig. 5. When 4-CP aqueous solutions are used, at the natural pH (5.8), TiO_2 prepared by the solvothermal method is less efficient than the well-known P-25 catalyst. The Ce0.6Ti–O catalyst shows a slightly higher photoactivity at the early stages of the reaction. In the first 15 min, the 4-CP conversion is 50.1% for Ce0.6Ti–O against the 38.4% obtained with P-25. However, after this period, the activity of Ce0.6Ti–O decreases considerably when compared with P-25, namely 86.6% of 4-CP abatement is achieved in 180 min with Ce0.6Ti–O while total disappearance of 4-CP is observed for P-25.

The BET surface areas of Ce0.2–Ti–O, Ce0.6–Ti–O and TiO_2 P-25 are 105, 124 and 47 m^2/g, respectively. Regarding the Ce-doped TiO_2 materials, it was observed that a slight increase in the surface area of the photocatalysts resulted in an increase in the photodegradation efficiency. Nevertheless, TiO_2 P-25, that has a much lower surface area, shows higher efficiency in the photodegradation of 4-CP than Ce0.2–Ti–O, thus showing that the surface area is not the key factor responsible for the photo-efficiency of the catalysts.

It is noteworthy to observe that by changing the pH of the initial solution to 10, Ce0.6Ti–O is more active than P-25; both catalysts reach nearly 100% of 4-CP conversion in 120 min. The point of zero charge (pzc) of TiO_2 and Ce-doped TiO_2 materials is 6.0–6.8 [4,22–26] and the pK_a of 4-CP is 9.41 [27]. In the alkaline media, the catalyst become negatively charged and the ionization state of the catalyst surface may play an important role as it can affect, for example, the degree of adsorption of organic matter on the surface. Blank experiments in the dark revealed that, regardless of the pH used, the amount of 4-CP adsorbed was never larger than 3% of its initial concentration indicating that adsorption is not important. The results suggest that during the initial reaction times, and for both pH values, Ce0.6Ti–O is more active than P-25, losing its higher activity after 15 min at natural pH. This can be explained considering that, at high pH, the chloride (Cl^-) anions released into the solution during the 4-CP degradation, are repulsed by the negatively charged catalyst surface. On the other hand, at low pH the chemical affinity of these anions with the TiO_2 surface increases [28], blocking the active sites of the catalyst. For this reason, in spite of the initial high activity at both pH values, for lower pH, as far as chloride ions are attached to the catalyst surface, deactivation occurs due to possible chlorination of the Ce0.6Ti–O catalyst, thus decreasing its activity.

In order to test this hypothesis, the used Ce0.6Ti–O catalyst was analyzed by HRTEM/EDXS after the reactions carried out at both pH values (results no shown). Chlorine (Cl) was not present in these samples, at least in quantity larger than 0.1% (w/w) (which is the detection limit of the technique). It is worth to note that analysis of the catalyst used at natural pH (5.8) revealed complete absence of ceria, consisting only on TiO_2. In contrast, ceria was found in the analysis of the TiO_2 matrix of the catalyst used at pH 10. In view of the observed results, it is possible to discard the effect of chlorination and consider that the loss of activity after 15 min, at natural pH, can only result from the disappearance of the ceria phase from the catalyst surface. This being the case, the beneficial effect of Ce-doping at pH 10, towards producing a catalyst more active than the common P-25 catalyst, is clear.

3.4. Reaction intermediates and mechanistic interpretation

There are different interpretations of the possible mechanisms that occur with Ce-doped TiO_2 catalysts: (i) the lanthanide ions interact directly with the organic molecules by means of the *f* orbital or (ii) the cerium-trapped electrons are efficiently transferred to the adsorbed O_2 to generate superoxide anion radicals $O_2^{\bullet -}$, which subsequently react with the organics [8,13].

In the experiments with the Ce-doped TiO_2 catalysts, two main intermediates were detected: hydroquinone (HQ) and benzoquinone (BQ), as represented in Fig. 6a and b, respectively. When P-25

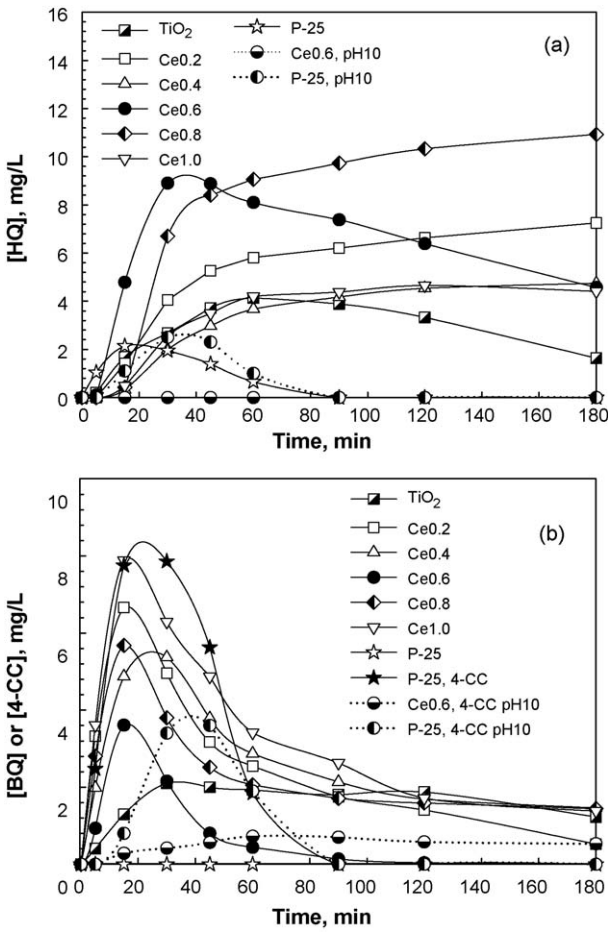

Fig. 6. Concentration–time curves of (a) HQ and (b) BQ (including 4-CC when indicated) during the photocatalytic experiments using different catalysts at natural pH (5.8) or adjusted to a pH value of 10 (when indicated by the figure label).

was tested, BQ was not present, trace amounts of HQ were detected and additionally 4-chlorocatechol (4-CC) was identified as one of the main intermediates (Fig. 6b). There are two reasons which can explain the absence of 4-CC with Ce-doped TiO_2: (i) the reaction mechanism with Ce-doped TiO_2 catalysts is different from the one related with P-25; or (ii) the significant deviations existing between the BET surface area of these materials (47 and 124 m^2/g for P-25 and Ce0.6Ti–O) influence the distribution of intermediates, since it is known that the adsorption constant of 4-CC is greater than that of HQ [21]. In light of the results obtained, the first hypothesis seems more reasonable, i.e. the reaction mechanisms are different, because: (a) the nature of these photocatalysts is different; (b) with P-25 the surface attack by $HO^{\bullet}$ radicals is the expected pathway of photocatalytic reactions of phenolic compounds [19], resulting in 4-CC formation preferentially to formation of BQ and HQ (in fact, BQ was not detected and the concentration of 4-CC obtained is much larger than the one detected for HQ); (c) since the lanthanide interacts strongly with the aromatic ring, direct oxidation of 4-CP through the electronic hole present on the particle surface, competes with $HO^{\bullet}$ (or $O_2^{\bullet -}$) surface reactions, leading to the preferential production of BQ and HQ main intermediates, in detriment of the chlorocatecholic route.

It is noteworthy to mention that, for a high pH, HQ was not formed with Ce0.6Ti–O (Fig. 6a), 4-CC was found in lower concentrations with P-25 (Fig. 6b) and BQ was not detected in both cases (not shown). Since the concentration of aromatic compounds decreases for a pH value of 10, these observations suggest that oxidation of 4-CP in basic solution occurs through 4-chlorophenoxide radical, which does not produce aromatic intermediates [29]. The concentration of chloride anions in solution was determined by ion chromatography. After 180 min, using the Ce0.6Ti–O catalyst, values of 4 and 19 mg/L were obtained for natural and basic solutions, respectively, in agreement with the higher 4-CP degradation observed at high pH. In the case of P-25 in basic solution, the concentration of chloride ions was 24 mg/L. Taking into account the initial concentration of 4-CP and considering that all the Cl is released in the form of Cl^-, the maximum amount of this ion that can be produced at the end of the reaction is 28 mg/L. Therefore, some non-identified Cl-containing species should be still present in the solution after 180 min, which are probably non-aromatic compounds, or simply Cl_2. When using the Ce0.6–Ti–O catalyst, Cl^- ions result from the direct dechlorination of 4-CP, while in the case of P-25 the dechlorination is driven through degradation of 4-CC.

4. Conclusions

Ce-doped TiO_2 materials prepared by a solvothermal method were successfully used in the photocatalytic conversion of 4-CP under visible irradiation. Ceria effectively shifts the TiO_2 absorption edge towards longer wavelengths, by reducing the band gap of the original material. Additionally, the presence of cerium retards TiO_2 transition from amorphous to crystalline anatase form. Both factors contribute for increased photocatalytic performance. An optimal Ce doping concentration exists and is 0.6% (w/w).

The main mechanism of catalyst deactivation is ceria loss from the catalyst surface during reaction. This process is pH dependent. At an initial pH of 10, Ce0.6Ti–O was photocatalytically more active than P-25 during the entire experiment and deactivation was not observed.

In 4-CP conversion, the $HO^{\bullet}$ attack of the chlorophenolic molecule must be the preferred mechanistic pathway when using the P-25 catalyst, while with Ce-doped catalysts direct oxidation through electron hole, present on the surface, must be considered. As the pH increase, the contribution of the latter route diminishes.

Acknowledgements

The authors acknowledge Fundação para a Ciência e Tecnologia of Portugal (projects POCI/N010/2006, SFRH/BD/16966/2004, POCTI/58252/EQU/2004) and the Ministry of Higher Education, Science and Technology of Slovenia, for financial support under the Portugal-Slovenia Cooperation in Science and Technology 2008-2009. GD acknowledges the financial support of the Slovenian Research Agency. The authors wish to thank Degussa A.G. (now Evonik) for providing the catalyst, Dr. Rui Boaventura for the analysis of chlorides and Dr. Pedro Tavares (UTAD, Universidade de Trás-os-Montes e Alto Douro) for the XRD analysis.

References

[1] Commission of the European Communities, Directive of the European Parliament and of the Council on environmental quality Standards in the field of water policy and amending Directive 2000/60/EC, COM (2006) 397 Final, Brussels, July 2006.
[2] J.-M. Herrmann, Top. Catal. 34 (2005) 49.
[3] S. Malato, J. Blanco, D.C. Alarcón, M.I. Maldonado, P. Fernández-Ibáñez, W. Gernjak, Catal. Today 122 (2007) 137.
[4] I.K. Konstantinou, T.A. Albanis, Appl. Catal. B: Environ. 49 (2004) 1.
[5] H. de Lasa, B. Serrano, M. Salaices, Photocatalytic Reaction Engineering, Springer, New York, 2005.
[6] A. Mills, S.-K. Lee, J. Photochem. Photobiol. A 152 (2002) 233.
[7] B. Ohtani, Chem. Lett. 37 (2008) 217.
[8] F.B. Li, X.Z. Li, M.F. Hou, K.W. Cheah, W.C.H. Choy, Appl. Catal. A: Gen. 285 (2005) 181.
[9] C. Liu, X. Tang, C. Mo, Z. Qiang, J. Solid State Chem. 181 (2008) 913.
[10] T. Tong, J. Zhang, B. Tian, F. Chen, D. He, M. Anpo, J. Colloids Interf. Sci. 315 (2007) 382.
[11] Z. Liu, B. Guo, L. Hong, H. Jiang, J. Phys. Chem. Solids 66 (2005) 161.
[12] J. Xiao, T. Peng, R. Li, Z. Peng, C. Yan, J. Solid State Chem. 179 (2006) 1161.
[13] Y. Xie, C. Yuan, Appl. Catal. B: Environ. 46 (2003) 251.
[14] Y. Xu, H. Chen, Z.-X. Zeng, B. Lei, Appl. Surf. Sci. 252 (2006) 8565.
[15] G. Li, C. Liu, Y. Liu, Appl. Surf. Sci. 253 (2006) 2481.
[16] M. Pera-Titus, V. García-Molina, M.A. Baños, J. Giménez, S. Esplugas, Appl. Catal. B: Environ. 47 (2004) 219.
[17] J.R.S. Brownson, M.I. Tejedor-Tejedor, M.A. Anderson, Chem. Mater. 17 (2005) 6304.
[18] B.D. Stojanovic, Z.V. Marinkovic, G.O. Brankovic, E. Fidancevska, J. Therm. Anal. Calorim. 60 (2000) 595.
[19] A. Di Paola, V. Augugliaro, L. Palmisano, G. Pantaleo, E. Savinov, J. Photochem. Photobiol. A 155 (2003) 207.
[20] A.M.T. Silva, E. Nouli, N.P. Xekoukoulotakis, D. Mantzavinos, Appl. Catal. B: Environ. 73 (2007) 11.
[21] C. Guillard, J. Disdier, J.-M. Herrmann, C. Lehaut, T. Chopin, S. Malato, J. Blanco, Catal. Today 54 (1999) 217.
[22] C.G. Silva, W. Wang, J.L. Faria, J. Photochem. Photobiol. A 181 (2006) 314.
[23] Y.X. Chen, K. Wang, L.P. Lou, J. Photochem. Photobiol. A 163 (2004) 281.
[24] H.H. Habibi, A. Hassanzadeh, S. Mahdavi, J. Photochem. Photobiol. A 172 (2005) 89.
[25] C.-H. Wu, C.-L. Chang, J. Hazard. Mater. B128 (2006) 265.
[26] J. Lin, J.C. Yu, J. Photochem. Photobiol. A 116 (1998) 63.
[27] David R. Lide, CRC Handbook of Chemistry and Physics, 88th edition (Internet Version 2008), CRC Press/Taylor and Francis, Boca Raton, Fl.
[28] D. Gumy, S.A. Giraldo, J. Rengifo, C. Pulgarin, Appl. Catal. B: Environ. 78 (2008) 19.
[29] U. Stafford, K.A. Gray, P.V. Kamat, J. Phys. Chem. 98 (1994) 6343.